17th World Conference on Earthquake Engineering, 17WCEE
Sendai, Japan - September 13th to 18th 2020

SHAKE TABLE TESTS OF A THREE-STOREY STRUCTURE WITH AN INERTER-BASED-HYSTERETIC-DAMPER

P. Deastra[(1)], D. J. Wagg[(2)], N. D. Sims[(3)], R. S. Mills[(4)]

[(1)] *PhD student, Department of Mechanical Engineering University of Sheffield, pdeastra1@sheffield.ac.uk*
[(2)] *Professor, Department of Mechanical Engineering University of Sheffield, david.wagg@sheffield.ac.uk*
[(3)] *Professor, Department of Mechanical Engineering University of Sheffield, n.sims@sheffield.ac.uk*
[(4)] *Technical Engineering Team Leader, Laboratory for Verification and Validation University of Sheffield, robin.mills@sheffield.ac.uk*

Abstract

Inerters have received substantial interest from the earthquake engineering community, because of their potential to improve the seismic isolation of structures. An inerter generates a force proportional to the relative acceleration across the two terminals of the device; this is in contrast to a pure mass which has one terminal and generates a force proportional to absolute acceleration. In practice the realization of an ideal inerter is very difficult, because of the inevitable influence of parasitic characteristics such as mass, damping, and (depending on the design) stiffness that are not considered in a lumped-parameter representation. The present study explores the potential of an alternative inerter design that minimizes the friction damping in the device, thereby seeking to reduce the parasitic damping within the vibration isolation system. The inerter is comprised of a flywheel and linear guideway mechanism. The center of the flywheel acts as one of the inerter terminals and at the same time is also the center of its rotation. The other terminal of the inerter is on the linear slider. Thus, the inertance generated is proportional to the relative acceleration between these two points. Unlike a traditional ball-screw inerter, this new design allows the inertance to be easily adjusted by changing the distance between the two terminals. The inerter is connected in series to a hysteretic material damper to form an inerter-based-hysteretic-damper (IBhD). Two linear mathematical models are proposed for the IBhD device, namely a tuned-inerter-hysteretic-damper (TIhD) model and a tuned-mass-hysteretic-damper-inerter (TMhDI). Finally, shake table experiments of a 3-storey structure with a grounded IBhD were undertaken. Particular emphasis is given to the comparison between the two models with the experimental results. It was found that the TMhDI model gives a more accurate result for this IBhD device. Furthermore, the IBhD was proven to be able to reduce the structural response due to earthquakes. Specifically, the peak response acceleration of the top storey is reduced by 38.4% for Northridge and 20.3% for El Centro earthquake. Moreover, the root-mean-square (RMS) of the acceleration response is also reduced by 51.3% and 46.1% for Northridge and El Centro earthquakes respectively.

Keywords: Inerter; Shake-table; Flywheel; Tuned-inerter-hysteretic-damper; Tuned-mass-hysteretic-damper-inerter.

1. Introduction

The concept of using an inerter as a seismic control device for building structures has achieved special attention recently. This is due to the fact that the inerter can act as a mass amplifier by generating forces proportional to its two terminals' relative acceleration. For example, the inerter in [1] is capable of generating inertance of 700kg with only 3.5kg of physical mass. In its application, an inerter is often combined with stiffness and damping elements to form an inerter-based-damper (IBD). There are three particularly popular IBDs available in the literature, namely the tuned-inerter-damper (TID), the tuned-mass-damper-inerter (TMDI) and the tuned-viscous-mass-damper (TVMD) as shown in Figure 1. Here b, k_d, c_d and m_d are inertance, stiffness, viscous damping, and secondary mass of the IBD systems respectively.

In 2007, Saito et al. [2] introduced a new IBD called the TVMD. Its mathematical model consists of a parallel connected inerter-dashpot in series connection with a spring element. In 2014, Lazar et al. [3] proposed a TID consisting of a parallel connected spring-dashpot in series connection with an inerter. Its mechanical layout is very similar with a tuned-mass-damper (TMD) with the TMD mass is replaced by an inerter element.

The optimum tuning procedure based on the fixed-point theory was used to obtain the TID's stiffness and damping optimum parameters. The superiority of the TID in comparison with the TMD is that it can be designed to have a very large mass ratio with a relatively small physical mass. Furthermore, it has been shown that the optimum location of the TID is at the bottom storey level, between the first storey and the ground [3].

The TMDI was firstly introduced by Marian and Giaralis [4]. Similar with the TID, the TMDI is basically an improved TMD with an added inerter element to achieve a large mass ratio. The mechanical layout of the TMDI consists of a parallel connected spring-dashpot in series connection with a series connected mass-inerter elements. If the TMDI mass m_d is zero, it then becomes a TID. The use of TMDI for earthquake protection device in building structures has been extensively discussed in literature, for example see [5-7].

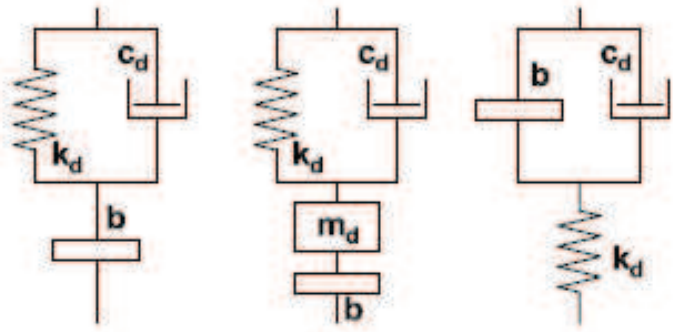

(a) (b) (c)

Fig. 1 – (a) TID (b) TMDI (c) TVMD

Despite of their promising performance as a seismic control device for building structures, only a few numbers of published works have presented the experimental validation of the IBDs, particularly the TID and the TMDI. The experimental work of the TMDI concept was firstly presented in [8]. Other experimental work on the IBDs devices are mostly employing the TVMD, for example see [9-14]. However, to the best of the authors' knowledge, the effectiveness of the TID and TMDI for controlling structural response of multi-storey building structures has never been experimentally explored in detail.

In this paper, for the first time a set of shake table experiments of a multi-storey structure with an inerter-based-hysteretic-damper (IBhD) installed between the first floor and the ground (table) is presented. Unlike the IBD, the IBhD has a hysteretic damping represented by a complex stiffness $k_d(1 + j\,\eta)$, where $j = \sqrt{-1}$, k_d is the stiffness of the IBhD, and η is the loss factor of the material. This is considered to be a more realistic model of the IBD systems when a material damping is present in the system. It should be noted that although the complex stiffness is a non-causal model, it has been widely used in practice [15] and can also be accurate and practical for design of structures employing non-linear dampers [16].

In this paper, two linear mathematical models are used to represent the IBhD device, namely tuned-inerter-hysteretic-damper (TIhD) and tuned-mass-hysteretic-damper-inerter (TMhDI). The layout of the TMhDI is similar to the TMDI with the viscous damping and spring elements replaced by a linear hysteretic damping given by a material damping represented by a complex stiffness. As a result, the TIhD is basically a TMhDI when the mass element m_d is zero. A more detailed discussion about TIhD and TMhDI concepts can be found in a separate paper by some of the authors, see [17].

2. Analytical models

The design parameters of the IBhD device in this paper were obtained based on a three-storey steel structure that has been built based on the layout shown schematically in Figure 2 (a). The analytical models of the TIhD and TMhDI devices are shown in Figure 2 (b) and 2 (c) respectively. Here m_i and $k_{n,l}$ are the mass of storey i and stiffness between storey n and l respectively and x_i is storey displacement of the i-th storey. The mass

© The 17th World Conference on Earthquake Engineering

element and inertance of the IBhD are denoted by m_d and b_d respectively. The hysteretic damper is represented by real (k_d) and imaginary (s_h) stiffness terms so that $\eta = s_h/k_d$.

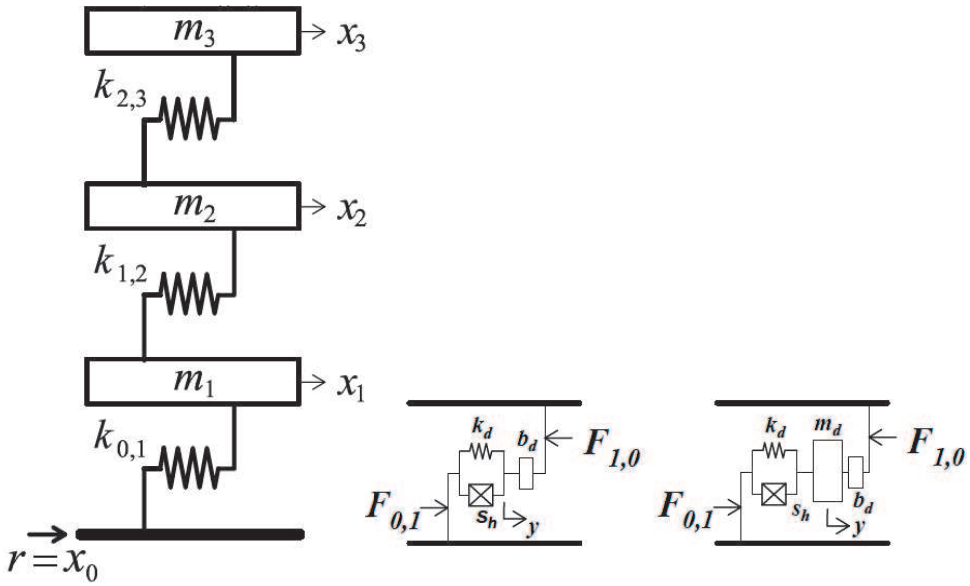

(a) (b) (c)

Fig. 2 – (a) A three-storey structure (b) TIhD (c) TMhDI

Table 1 – Structural properties of the structure

Storey	Mass (kg)	Stiffness (N/m)
1	33.15	1.4048 x 10^5
2	24.15	1.6858 x 10^5
3	24.15	2.0792 x 10^5

The properties of mass and stiffness of the structure are given in Table 1. For simplicity, the natural damping of the structure was assumed to be zero. The equation of motion of the structure with a grounded IBhD subject to a ground displacement can be written as

$$\begin{cases} (m_1 s^2 + k_{0,1} + k_{1,2})X_1 = k_{1,2}X_2 + k_{0,1}R + F_{1,0} \\ (m_2 s^2 + k_{1,2} + k_{2,3})X_2 = k_{1,2}X_1 + k_{2,3}X_3 \\ (m_3 s^2 + k_{2,3})X_3 = k_{2,3}X_2 \end{cases} \quad (1)$$

The ground displacement is denoted as r, which is also equal to the x_0 storey displacement. X_i and R are Laplace transformed versions of x_i and r respectively, $F_{1,0} = F_{0,1}$ is the IBhD force transferred into the structure in Laplace domain. For TIhD, $F_{1,0}$ is given by

$$F_{1,0} = \frac{b_d s^2 (k_d(1 + j\,\eta))}{b_d s^2 + k_d(1 + j\,\eta)}(R - X_1) \quad (2)$$

where s is the Laplace variable. For TMhDI, $F_{1,0}$ is given by

© The 17th World Conference on Earthquake Engineering

$$F_{1,0} = \frac{k_d(1+j\,\eta\,)\,b_d s^2}{(m_d+b_d)s^2+k_d(1+j\,\eta\,)}R + \frac{-(m_d+b_d)s^2 k_d(1+j\,\eta\,)}{(m_d+b_d)s^2+k_d(1+j\,\eta\,)}X_1 \tag{3}$$

3. Optimum design of the IBhD

Both the TIhD and TMhDI are tuned by targeting the first mode of the host structure. The optimization procedure is adopted from [17]. The obtained optimum parameters are given in Table 2.

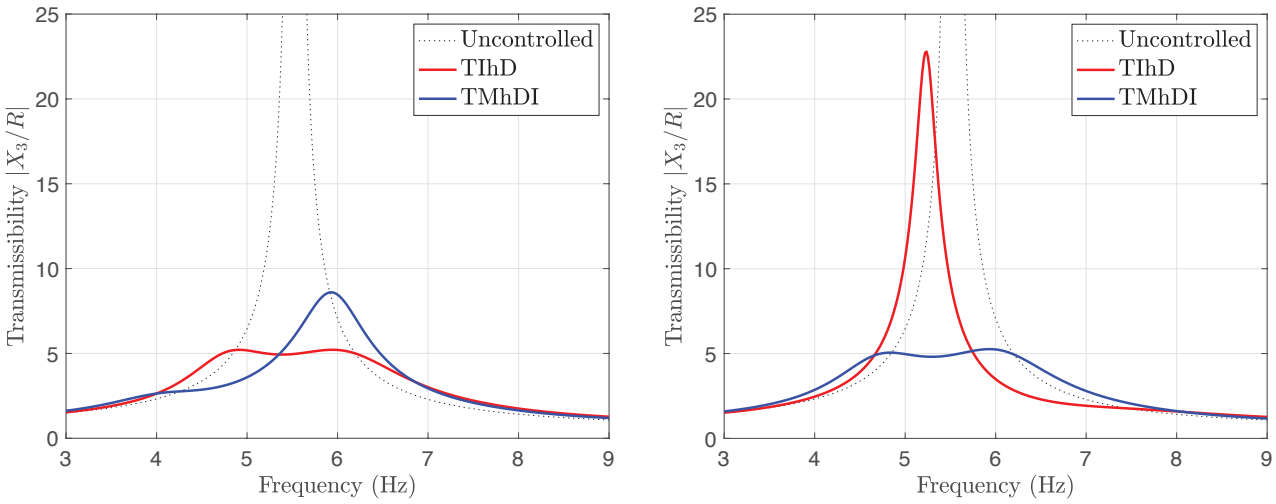

Fig. 3 – First resonance of structural response with TIhD and TMhDI with (a) m_d= 0 (b) m_d= 10kg

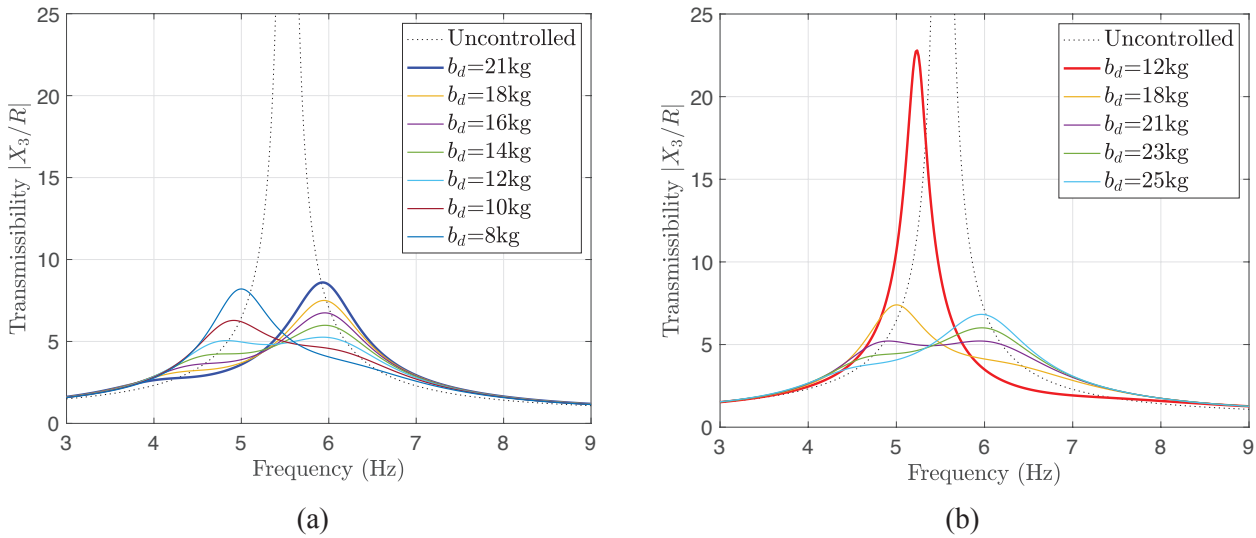

Fig. 4 – Effect of b_d on minimizing the mis-tuning of (a) TMhDI (b) TIhD

Figure 3 (a) and 3 (b) show the first resonance of the structural frequency response in the form of transmissibility from the ground to the top storey. Figure 3 (a) shows the response of the host structure with an optimized TIhD. It is also shown in this Figure the mis-tuning of the TMhDI when using the optimized parameters of the TIhD as given in Table 2. Similarly, Figure 3 (b) shows the structural response with an

© The 17th World Conference on Earthquake Engineering

optimized TMhDI and a mis-tuning of the TIhD due to the optimum parameters of the TMhDI are used as given in Table 2. It is obvious from these figures that inaccurate estimations of m_d could result in a mis-tuning of both TIhD and TMhDI.

Figure 3(a) is the case where b_d is optimized with m_d assumed to be zero (TIhD). As a result, if in fact m_d is significant and cannot be neglected, it could result in the actual behavior being that of a mis-tuned TMhDI. Similarly, Figure 3 (b) is the case where b_d is optimized with m_d is assumed to be non-zero (TMhDI), hence the mis-tuned TIhD if in fact m_d is close to zero. However, in reality the TMhDI is considered to be more realistic, because in most situations the mass of the inerter which is acting as m_d cannot be neglected. In both Figures k_d and η stay the same (k_d=22000N/m and η =0.53).

Figure 4 (a) and 4 (b) show how the mis-tuning of TIhD and TMhDI can be minimized by adjusting the inertance only and keeping the same material damping, meaning k_d and η stay the same. Figure 4 (a) shows the effect of changing inertance on the mis-tuned TMhDI from Figure 3 (a). It can be seen that by reducing the inertance the structural response can be reduced. However, after a certain level, it will increase to an even larger amplitude. Similarly, Figure 4 (b) shows how inertance can minimize the structural response due to the mis-tuning of the TIhD in Figure 3 (b). It is obvious that equal peaks can be achieved by changing the inertance to 21kg in this example.

In conclusion, it is suggested that m_d should not be ignored in the design of the IBhD paramerers in case the material damper is not adjustable. This is because it is easier to minimize the mis-tuning by changing the intertance parameters such that the two equal peaks can be achieved. Furthermore, because the inertance parameter can be useful to help the mis-tuned TIhD and TMhDI, it is better to design an adjustable inerter. The mis-tuning phenomenon can easily be caused by the effect of unmodeled influences, such as subtle changes in the boundary conditions of the structure or parasitic mass or damping within the vibration isolation system.

Table 2 – Optimum parameters of TIhD and TMhDI for a given b_d and m_d

Parameter	**Optimum value**	
	TIhD	**TMhDI**
Inertance, b_d (kg)	21	12
Stiffness, k_d (N/m)	22000	22000
Loss factor, η	0.53	0.53
Secondary mass, m_d (kg)	0	10kg

4. Design of inerter and damper

To achieve the optimum parameters of the IBhD given in Table 2, both inerter and material damper devices were designed and individually tested in the lab.

4.1 Inerter

In this paper a flywheel-type inerter was designed with minimum friction as can be seen in Figure 5. In this inerter, the translational relative motion from its two terminals is converted to a rotational motion of a flywheel via a linear guideway mechanism. Due to the absence of a ball-screw or rack and pinion, this design reduces the internal damping due to friction. The flywheel support is acting as one of the terminals of the inerter. Another terminal of the inerter is located on the linear slider connecting the flywheel with the damping material. Given that the distance between the two inerter terminals is l_a (lever arm), the inertance can be calculated by Eq. (4) assuming the lever arm rotation θ is small [18] using

$$b_d = \frac{I}{{l_a}^2} \tag{4}$$

© The 17th World Conference on Earthquake Engineering

where I is the inertia of the flywheel.

A set of experiments to characterize the inerter was conducted. As shown in Figure 5, the experimental rig consists of a flywheel inerter with fixed support acting as one terminal. The second terminal of the inerter is connected to a shaker. The shaker applies sinusoidal forces F to the flywheel measured by the force transducer. The second terminal of the flywheel will oscillate with acceleration of a_2 measured by the accelerometer. Finally, the actual inertance of the inerter was obtained by using the averaged values of b_d given in Eq. (5), where both $F(t)$ and $a_2(t)$ are sine waves.

$$b_d = \frac{F(t)}{a_2(t)} \tag{5}$$

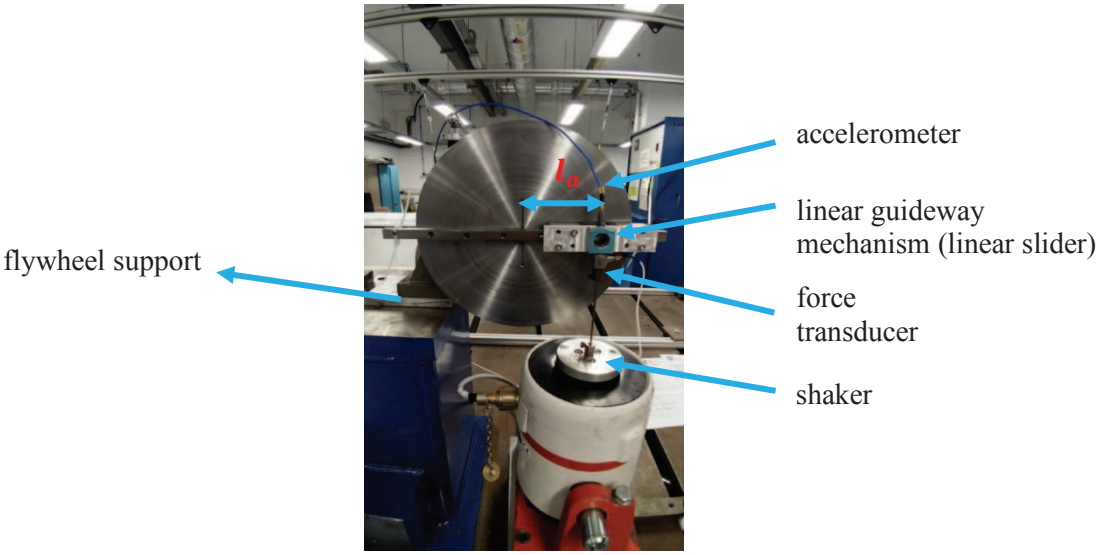

Fig. 5 – Flywheel inerter on an experimental rig

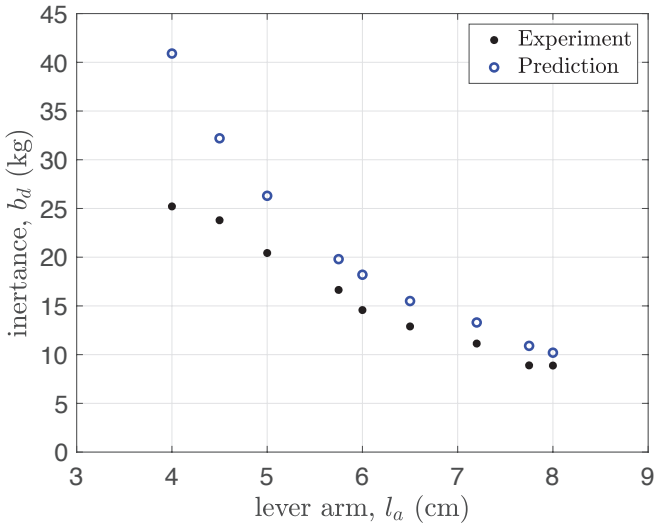

Fig. 6 – b_d versus l_a: Experiment (Eq.(5)) vs Predicted (Eq.(4))

Figure 6 shows the plot of b_d against l_a. The predicted results were obtained by Eq. (4) and the experimental results were obtained by Eq. (5). Overall the prediction and experiment are in a reasonably good agreement, particularly when l_a is large. Some discrepancies can be seen when l_a is small. This is logical,

© The 17th World Conference on Earthquake Engineering

because θ becomes large when l_a is small, hence the small angle assumption relating to Eq. (4) is no longer satisfied. It is also obvious from this Figure that the inerter is capable of generating inertance up to 25kg for the range of values tested. It should be noted that the actual mass of the flywheel is only 9kg which means in this case the inerter can generate inertance up to almost 3 times of its actual mass.

4.2 Material damper

A gel damper was designed to act as both k_d and η of the IBhD device. The gel was made from Magic Power Gel from Raytech. It consists of two components that can be mixed with different mixing ratio to achieved specific targeted parameters. The properties of the gel for different mixing ratio and various temperature conditions has been extensively discussed in [19].

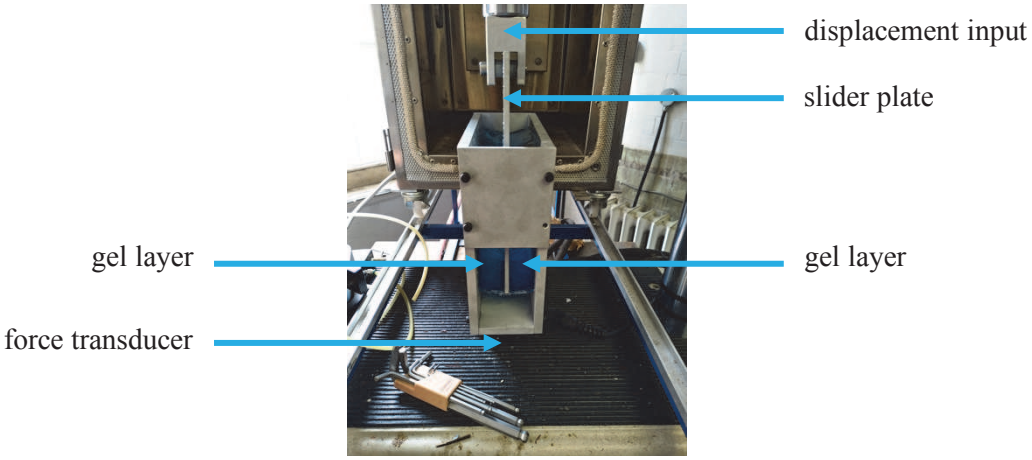

Fig. 7 – Gel damper on an experimental rig

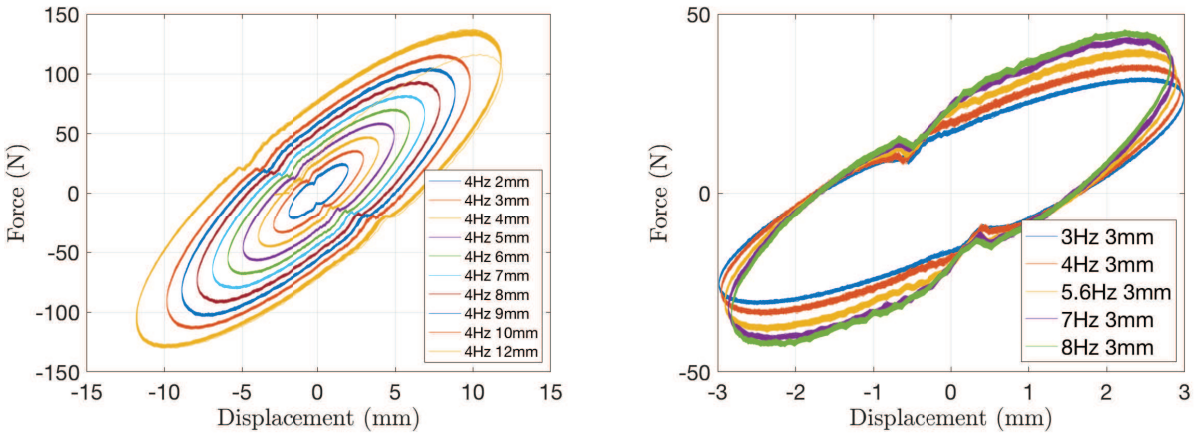

Fig. 8 – Hysteresis loop (a) fixed frequency, variable amplitude $f = 4$Hz (b) fixed amplitude, variable frequency $X = 3$mm

In this study, the gel mixing ratio is 1:1.058. Two gel dampers were built to be placed on both left and right-hand sides of the inerter, with a connection to the building structure. Each of the gel dampers consists of two gel layers separated by a slider plate. The gel dampers were then tested using the MTS servo-hydraulic load frame. The experimental test specimen can be seen in Figure 7. One end of the gel damper was fixed on a force transducer and another end was connected to the MTS servo-hydraulic load frame on the slider plate. The gel dampers were tested under sinusoidal displacement input signal with different frequencies f and

© The 17th World Conference on Earthquake Engineering

amplitudes X. The results are plotted in the form of force versus displacement hysteresis loops. Two representative plots are given in Figure 8 (a) and 8 (b).

From the hysteresis loops results, both k_d and η properties of the gel damper can be obtained. The stiffness is given by the slope of the loop, while the loss factor is given by Eq. (6) [20].

$$\eta = \frac{\Delta W}{\pi k_d X^2} \tag{6}$$

Here ΔW is the area inside of the hysteresis loop. Finally based on an averaged value of all the obtained hysteresis loops for the range of tested frequencies and input displacement amplitudes, the properties of the gel damper were obtained as given in Table 3. The viscous damping coefficient c_d of the TMDI model is obtained from equivalent viscous damping [20]

$$c_d = \frac{k_d \eta}{\omega_n} \tag{7}$$

where ω_n is the first natural frequency of the host structure.

Table 3 – Properties of the two gel dampers obtained from experiments

Parameter	Obtained value
Stiffness, k_d (N/m)	20000
Loss factor, η	0.53

4.3 IBhD device

The realization of the IBhD was achieved by combining the inerter and the gel dampers (coupled spring-damper) in series. Both the inerter and the two gel dampers were installed between the first storey of the structure and the ground (table). The first terminal of the inerter was fixed on a stiff frame system and another terminal of the inerter is connected to both gel dampers on the left and right sides via a beam. A handle was designed to enable the flywheel to be moved up and down (adjusting l_a). The photograph of this system is given in Figure 9.

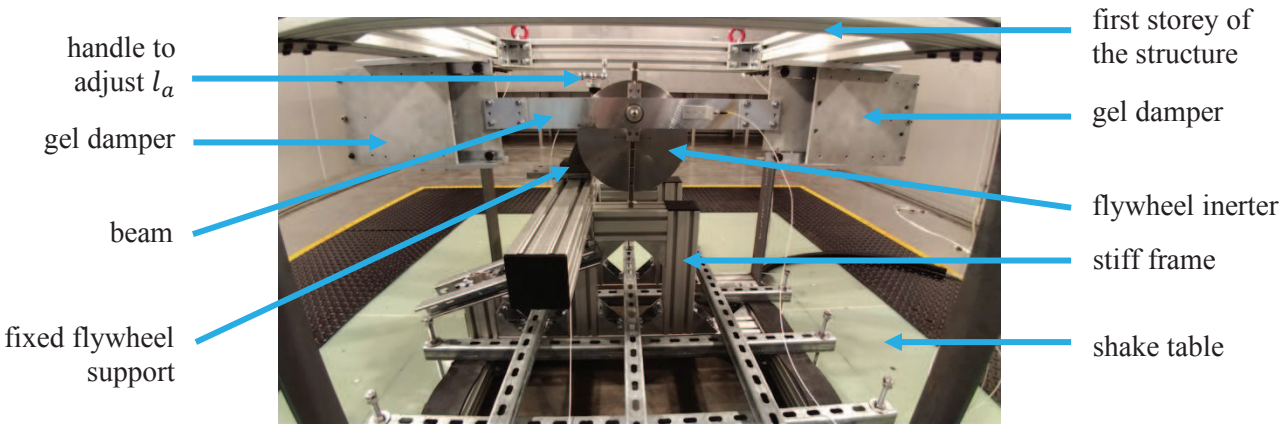

Fig. 9 – IBhD device

© The 17th World Conference on Earthquake Engineering

5. Shake table experimental set-up

The structure was built on a shake table system in the Laboratory for Verification and Validation (LVV) at the University of Sheffield with the IBhD device installed between the first storey and the table as shown in Figure 10. The shake table is a 6-degree of freedom integrated Multi Axis Shaker table system with 3m x 2m dimension. A set of experimental tests consisting of harmonic and seismic excitations was designed to investigate the effectiveness of the IBhD device in reducing the structural response of the host structure.

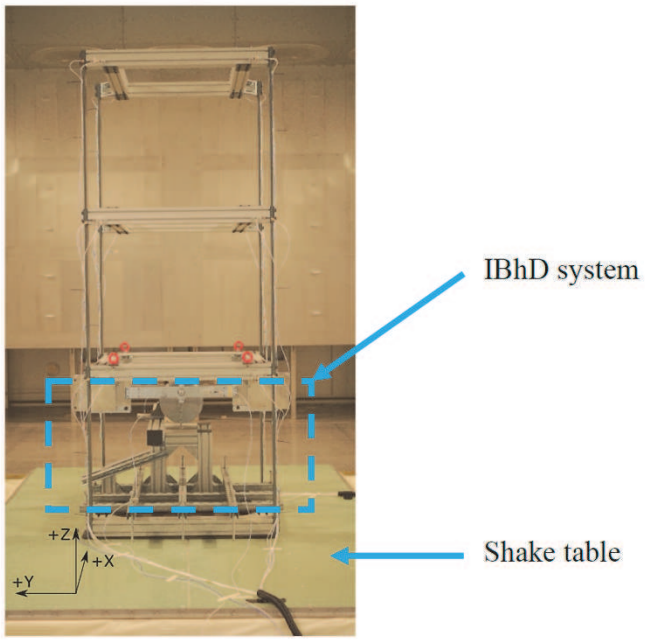

Fig. 10 – A three-storey structure with a grounded IBhD device

The tests were performed in the y-axis only. Accelerometers were placed on each storey to record the acceleration response of the structure. Based on hammer test results, a set of sine wave acceleration signals with frequency around the first resonant mode were prepared. For the seismic case, two different earthquakes with different frequency characteristics were used for the experiments. The Northridge and El Centro earthquakes were selected representing broad-band and narrow-band frequency earthquakes respectively. It should be noted that both earthquakes signals were frequency shifted such that the predominant frequency of maximum energy coincided with the first resonance of the structure. These modified signals were then band-filtered to pass between 3Hz and 70Hz. This is because the risk of running the shake table at frequency below 3Hz would coincide with the natural frequency of the support structure of the shake table system. However, this modification does not significantly change the nature of the earthquake in terms of their frequency and time domain shape characteristic and their peak ground acceleration (PGA).

6. Results and discussion

6.1 Harmonic base excitation

The first part of the experiment is harmonic base excitations. The input signal was a set of sine wave acceleration signals with frequency around the first resonance and amplitude ranging from 1m/s^2 to 25m/s^2. The lever arm l_a of the inerter was set to be 55mm. The results are compared with the models as shown in Figure 11. Overall, both the uncontrolled structure and the structure with an IBhD analytical models are in a relatively good agreement with the experiment. In particular the TMhDI model shows a better agreement with the experiment compare to the TIhD model. This supports the assumption that the mass element m_d cannot be

© The 17th World Conference on Earthquake Engineering

neglected for this system. In this experiment, m_d is the mass of the flywheel inerter plus the mass of the beam which is estimated to be 10kg.

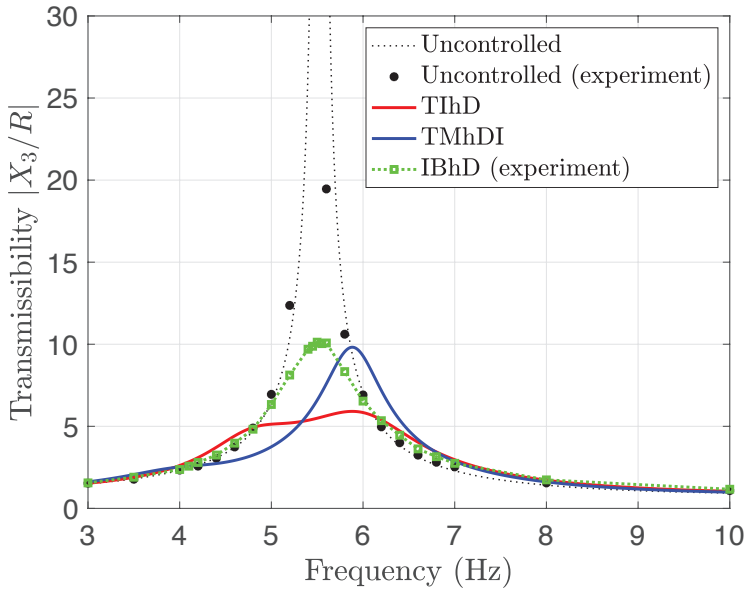

Fig. 11 – Structural response transmissibility: Comparison of analytical models and experimental results

It should be noted, this is not the optimum TMhDI due to the mis-tuning during the design process of the gel dampers. The actual k_d of the gel damper is found to be less than expected. Theoretically, in order to minimize the mis-tuning the inertance should be adjusted by changing the lever arm l_a of the flywheel inerter. However, in this experiment the l_a was fixed to 55mm.

6.2 Seismic base excitation

Following the successful harmonic base acceleration experiment, the effectiveness of the IBhD was also observed for seismic base excitations. Two different earthquakes as discussed in Section 5 were selected. The results are shown in Figure 12.

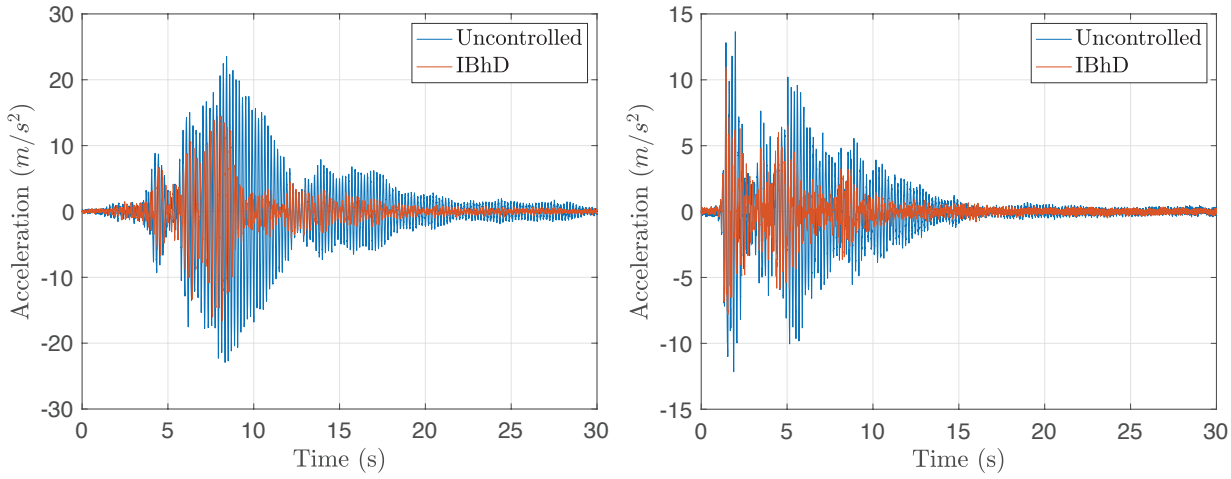

Fig. 12 – Experimental test results showing structural response of the top storey acceleration to earthquake base excitation in the x direction: (a) Northridge (b) El Centro

© The 17th World Conference on Earthquake Engineering

Figure 12 shows the structural response to two earthquakes with different frequency characteristic. Both Figure 12 (a) and (b) show that the IBhD can effectively reduce the structural response, which in this case is taken to be the top storey acceleration of the building structure. The peak response acceleration is reduced by 38.4% for Northridge and 20.3% for El Centro earthquake. The root-mean-square (RMS) of the acceleration response is also reduced by 51.3% and 46.1% for Northridge and El Centro earthquakes respectively. It should be noted that the IBhD parameters were still not optimum due to the mis-tuning as discussed in the previous section. It is expected that the structural performance can be further improved with an optimized IBhD device.

7. Conclusion

An example of an experimental realization of an IBhD is presented in this paper. The device combines two gel dampers and a flywheel inerter in series. A set of shake table experiments was carried out in order to assess the design methodology of this type of IBhD device. The IBhD was designed and optimized by using the fixed points method and targeting the first resonant mode of the host structure. The shake table experiments consisting of both harmonic and seismic base accelerations was performed in the Laboratory for Verification and Validation (LVV) of The University of Sheffield using a 3-storey scale model of a building as the test structure.

Two linear mathematical models were proposed for use in the design of the IBhD device and the results were compared with the experimental results. The first model assumes the secondary mass element m_d is zero, while the second model assumes it is not zero. The first and the second models are called TIhD and TMhDI respectively. Both models are compared with the shake table experimental results. It was shown that the TMhDI model gives a better agreement with the experimental result compared to the TIhD model, which supports the assumption that the mass of the IBhD device should not be neglected. Furthermore, shake table experiments were also performed by using two different earthquakes input base excitation. The results show that the IBhD can significantly reduce the peak response acceleration of the top storey structure, in this specific example, by 38.4% for Northridge and 20.3% for El Centro earthquake. It is expected that the reduction of the structural response can be even larger with optimum properties of the IBhD.

8. Acknowledgement

This work was supported by the Indonesia Endowment Fund for Education (LPDP), and the Engineering and Physical Sciences Research Council (grant numbers EP/J013714/1 and EP/N010884/1). The authors would like also to thank Michael J Dutchman and Mathew J Hall for their help on manufacturing and testing the IBhD components.

9. References

[1] Papageorgiou C, Houghton NE, Smith MC (2009): Experimental testing and analysis of inerter devices. *Journal of Dynamic Systems, Measurement, and Control*, **131** (1): 011001.

[2] Saito K, Kurita S, Inoue N (2007): Optimum response control of 1-DOF system using linear viscous damper with inertial mass and its Kelvin-type modelling. (in Japanese) *Journal of Structural Construction Engineering Architectural Institute of Japan*, **53B**: 53-66.

[3] Lazar IF, Neild SA, Wagg DJ (2014): Using an inerter-based device for structural vibration suppression. *Earthquake Engineering & Structural Dynamics,* **43**: 1129-1147

[4] Marian L, Giaralis A (2014): Optimal design of a novel tuned mass-damper-inerter (TMDI) passive vibration control configuration for stochastically support-excited structural systems. *Probabilistic Engineering Mechanics,* **38**: 156-164

[5] Pietrosanti D, De Angelis M, Basili M (2017): Optimal design and performance evaluation of systems with Tuned Mass Damper Inerter (TMDI). *Earthquake Engineering & Structural Dynamics*, **46**(8): 1367–1388

© The 17th World Conference on Earthquake Engineering

[6] De Domenico D, Ricciardi G (2017): An enhanced base isolation system equipped with optimal tuned mass damper inerter (TMDI). *Earthquake Engineering & Structural Dynamics*, **47**(5):1169–1192

[7] De Angelis M, Giaralis A, Petrini F, Pietrosanti D (2019): Optimal tuning and assessment of inertial dampers with grounded inerter for vibration control of seismically excited base-isolated systems. *Engineering Structures*, **196**:109250

[8] Brzeski P, Lazarek M, Perlikowski P (2017): Experimental study of the novel tuned mass damper with inerter which enables changes of inertance. *Journal of Sound and Vibration*, **404**: 47-57

[9] Ikago K, Saito K, Inoue N (2012): Seismic control of single-degree-of-freedom structure using tuned viscous mass damper. *Earthquake Engineering & Structural Dynamics*, **41**(3): 453–474

[10] Watanabe Y, Ikago K, Inoue N, Kida H, Nakaminami S, Tanaka H, Sugimura Y, Saito K (2012): Full-scale dynamic tests and analytical verification of a force-restricted tuned viscous mass damper. *Proceeding of the 15th World conference on earthquake engineering.* Lisboa, Portugal.

[11] Sugimura Y, Goto W, Tanizawa H, Saito K, Ninomiya T, Nagasaku T, Saito K (2012): Response control effect of steel building structure using tuned viscous mass damper. *Proceeding of the 15th World Conference on Earthquake Engineering.* Lisboa, Portugal.

[12] Ikago K, Ikenaga M, Nakaminami S, Saito K, Inoue N (2014): Shake table tests for a base-isolated system containing a rotary inertial damper. *Proceeding of the 12th International Conference on Computational Structures Technology*. Naples, Italy.

[13] Nakaminami S, Kida H, Ikago K, Inoue N (2017): Dynamic Testing of a full-scale hydraulic inerter-damper for the seismic protection of civil structures. *Proceeding of the 7th International Conference on Advances in Experimental Structural Engineering*. Pavia, Italy.

[14] Ikago K, Taniguchi S, Ikenaga M, Nakaminami S, Inoue N, Saito K (2017): An experimental study on the robustness of a tuned viscous mass damper system incorporated into a single-degree-of-freedom structure. *Proceeding of the 7th International Conference on Advances in Experimental Structural Engineering*. Pavia, Italy.

[15] Beards CF (1996): *Structural Vibration*. Butterworth-Heinemann,1st edition

[16] Inaudi JA, Kelly JM (1992): A friction mass damper for vibration control. *Earthquake Engineering Research Centre, University of California at Barkeley.* Report No.UCB/EERC-92/18

[17] Deastra P, Wagg DJ, Sims ND, Akbar M: Tuned inerter dampers with linear hysteretic damping. *Earthquake Engineering & Structural Dynamics (In Press).*

[18] John EDA, Wagg DJ (2019): Design and testing of a frictionless mechanical inerter device using living-hinges. *Journal of the Franklin Institute*, **356**: 7650-7668

[19] Almagirby A, Rongong JA, Carré MJ (2017): The development of a new artificial model of a finger for assessing transmitted vibrations. *Journal of the Mechanical Behavior of Biomedical Materials*, **78**: 20-27

[20] Rao SS (2011): *Mechanical Vibrations.* Pearson, 5th edition.

© The 17th World Conference on Earthquake Engineering